Published in final edited form as:
J Phys Chem Lett. ; 3(15): 1974–1979. doi:10.1021/jz300802k.

Probing the Structure and Chemistry of Perylenetetracarboxylic Dianhydride on Graphene Before and After Atomic Layer Deposition of Alumina

James E. Johns, **Hunter J. Karmel**, **Justice M. P. Alaboson**, and **Mark C. Hersam***
Departments of Materials Science and Engineering, Chemistry, and Medicine, Northwestern University, Evanston IL, 60208-3108, USA

Abstract

The superlative electronic properties of graphene suggest its use as the foundation of next generation integrated circuits. However, this application requires precise control of the interface between graphene and other materials, especially the metal oxides that are commonly used as gate dielectrics. Towards that end, organic seeding layers have been empirically shown to seed ultrathin dielectric growth on graphene via atomic layer deposition (ALD), although the underlying chemical mechanisms and structural details of the molecule/dielectric interface remain unknown. Here, confocal resonance Raman spectroscopy is employed to quantify the structure and chemistry of monolayers of 3,4,9,10-perylenetetracarboxylic dianhydride (PTCDA) on graphene before and after deposition of alumina with the ALD precursors trimethyl aluminum (TMA) and water. Photoluminescence measurements provide further insight into the details of the growth mechanism, including the transition between layer-by-layer growth and island formation. Overall, these results reveal that PTCDA is not consumed during ALD, thereby preserving a well-defined and passivating organic interface between graphene and deposited dielectric thin films.

Keywords

Graphene; Raman Spectroscopy; Surface Chemistry; Atomic Layer Deposition; Scanning Tunneling Microscopy; PTCDA

Manuscript

With exceptional charge carrier mobility and thermal conductivity, graphene is a promising electronic material for high frequency electronics. In research laboratories, graphene-based transistors have already shown charge carrier mobilities in excess of 200,000 cm^2/Vs[(1)] and operating frequencies higher than 100 GHz.[2] However, to maximize technological impact, these outstanding electrical properties need to be realized in wafer-scale, individually addressable, top-gated devices and circuits. The first step towards this goal is the development of methods for uniformly depositing ultrathin metal oxide dielectrics with well-defined interfaces on graphene.

*Corresponding Author: m-hersam@northwestern.edu.

ASSOCIATED CONTENT
Additional content related to sample preparation, experimental details, and supplementary spectroscopic information can be found in the Supporting Information. This material is available free of charge via the Internet at http://pubs.acs.org.

Author Contributions
All authors have contributed and given approval to this manuscript.

The deposition of thin films on graphene is complicated by the chemical inertness of the graphitic basal plane, which prevents uniform nucleation and growth.[3-4] Unlike many conventional electronic materials, graphene does not spontaneously form a native surface oxide which can promote additional surface chemistry. As a result, atomic layer deposition (ALD) of metal oxides nucleates inhomogeneously at step edges and defects, leading to poorly defined interfaces and high pinhole densities that causes undesirably high leakage currents.[3-4] Metal-oxide dielectrics on graphene can be successfully grown by other methods such as e-beam evaporation or ozone pretreatments, but these methods can introduce defects in the graphene lattice[5-6] and can reduce charge carrier mobility.[7]

Recently, it has been shown that uniform high-*k* dielectric films can be deposited by employing organic self-assembled monolayers as ALD seeding layers on graphene. For example, Wang *et al.* deposited an organic layer of perylenetetracarboxylic acid on a single graphene flake, and then successfully coated the surface with a conformal film of ALD alumina.[3] Alaboson *et al.* extended this technique to vapor deposited 3,4,9,10-perylenetetracarboxylic dianhydride (PTCDA) on epitaxial graphene (EG) on silicon carbide.[8] This latter study showed that PTCDA seeding layers lead to uniform ALD growth of alumina on graphene, enabling the fabrication of metal-oxide-graphene capacitors with high capacitance in excess of 700 nF/cm^2 with concurrently low leakage currents of 5×10^{-9} A/cm^2.[8]

Despite the empirical successes of these perylene-based seeding layers, the underlying chemistry, structure, and bonding between the ALD oxide and the molecular layer have not been quantitatively characterized. Typically, ALD reactions proceed via surface hydroxyl groups. However, since PTCDA does not present hydroxyl functionalization,[9] it is unclear whether ALD precursors attack the terminal carbonyls, the anhydrous oxygens, the perylene core of PTCDA, or require physisorbed water for the reaction to occur. Direct reaction of PTCDA with ALD precursors could leave charged molecular fragments behind, which would likely be detrimental to the performance of electronic devices due to increasing Coulomb scattering. Furthermore, charge transfer between PTCDA and graphene[10] may be influenced by chemical reactions that occur during ALD. Therefore, from both fundamental and applied perspectives, a detailed understanding of organic ALD seeding layers on graphene is of high interest.

Due to its propensity to self-assemble into ordered monolayers, PTCDA has been studied on a wide variety of surfaces.[11-14] Raman spectroscopy studies have measured the interactions and charge transfer of PTCDA on silver and semiconducting surfaces.[14-15] In particular, specific vibrational “reporter” modes of the perylene core have been identified as having a frequency shift that depends on the degree of charge transfer into or out of the PTCDA film. Vibrational modes that involve the carbonyl and anhydride functional groups are also detectable, allowing the detection of chemical reactions with the periphery of the molecule. The broad optical absorption spectrum of PTCDA films in the visible between 425 nm and 600 nm also enables resonance enhancement of the Raman signal even in the presence of substrate-induced dielectric shifts.[16] Furthermore, recent work suggests that the presence of graphene surfaces allow further improvements in the sensitivity of Raman measurements.[17]

Herein, we employ resonance Raman spectroscopy to study PTCDA monolayers on graphene before and after reaction with the ALD precursors trimethyl aluminum (TMA) and H_2O. Preceding ALD, we confirm the deposition and structure of PTCDA on graphene using scanning probe microscopy and resonance Raman spectroscopy, and then identify several reporter vibrational modes in PTCDA that confirm the presence of specific functional groups including the perylene core, anhydrous oxygen, and carbonyl groups. By comparing the Raman spectra before and after ALD, PTCDA is observed to survive the

growth of alumina films, which suggests that ALD is nucleated by physisorbed water as opposed to covalently reacting with PTCDA. We also investigate the intensity and spectral shift of perylene-based vibrational modes to probe charge transfer from the graphene into the molecular layer and spectral enhancement due to the presence of graphene.

The structure of PTCDA on EG on SiC(0001) is shown in Figure 1. Briefly, PTCDA is thermally evaporated onto EG in accordance with previously reported methods[18] and subsequently imaged in a home-built ultrahigh vacuum (UHV) scanning tunneling microscope (STM).[19] Additional details related to sample preparation are given in the Supporting Information. PTCDA uniformly coats the surface of graphene by forming a stable hydrogen-bonded network.[18,20-21] This stabilization allows the PTCDA domains to extend seamlessly over step edges, point defects, and one-dimensional defects without significant alteration to its crystallinity.[18] The expected herringbone structure of the PTCDA monolayer is observed in the high-resolution image of Figure 1d. The PTCDA unit cell dimensions from the STM image are 21.7 ± 0.1 Å × 12.6 ± 0.1 Å. It should be noted that this unit cell is not commensurate with the underlying graphene lattice, in contrast to the slightly contracted commensurate unit cell used in theoretical calculations by Tian *et al.* that showed charge transfer at the graphene/PTCDA interface.[10]

Following deposition of PTCDA, Raman spectra were recorded using the 514.5 nm line from an Ar^+ ion laser. Details of the spectrometer and data acquisition are given in the Supporting Information. Figure 2a and 2b show the Raman spectra for pristine EG, and with 1, 2, and 3 monolayer equivalents of PTCDA. Before deposition, all peaks are attributable to either graphene or silicon carbide. The largest SiC peaks are located at 767, 788, and 967 cm^{-1}, with combination and overtone bands in the 1520 to 1760 cm^{-1} range in agreement with previously reported values for n-doped 6H-SiC.[22] Spectral peaks assigned to graphene phonons can be seen at 1370 cm^{-1} (D band), 1598 cm^{-1} (G band), and 2720 cm^{-1} (2D band). The G and 2D bands are red-shifted from their nominal values for free standing graphene due to doping from the substrate and substrate-induced strain, respectively.[23]

Once PTCDA has been deposited, both the graphene peaks and the SiC overtone/combination band region are overwhelmed in intensity by the PTCDA Raman signal. The spectra after PTCDA deposition shown in Figure 2 have the substrate spectrum subtracted to more easily identify the PTCDA features. Table 1 lists the measured frequencies and relative intensities of the known PTCDA Raman peaks, and references them to their single crystal values. The listed intensities were normalized to the most intense PTCDA peak at 1306 cm^{-1}.

All of the Raman peaks measured in this study match closely with those for crystalline PTCDA. In particular, the peak corresponding to a C-H bend at 1306 cm^{-1} is similar to the value reported by Scholz (1304.8 cm^{-1})[13] and by Akers for thin films (1304 cm^{-1})[25], in which each molecule is electrically neutral. In contrast, ultrathin films in which there is strong charge transfer between the substrate and PTCDA, such as PTCDA on Ag(111)[14] or annealed submonolayers of PTCDA on Si(001)[15], show a marked decrease in the Raman shift of this mode due to charge transfer and substrate interactions. The ability of this mode to serve as a reporter of charge transfer has also been confirmed theoretically by Kobitski *et al.* who calculated a spectral shift in this mode of −18 cm^{-1}/e^- and −16 cm^{-1}/e^- for the cation and anion respectively.[15] Here, we find no evidence to support any substantial charge transfer between graphene and PTCDA.

A photoluminescent (PL) background is absent from the PTCDA monolayer spectrum, but appears as the coverage increases. This observation is consistent with the expected layer-by-layer growth of PTCDA on graphene for the first two monolayers,[20] and the associated

fluorescence quenching resulting from the semi-metallic nature of graphene. The addition of a second monolayer shows a small increase in PL, and by 3 monolayer equivalents, a clear PL background is present beyond 1200 cm^{-1}, which is consistent with previously reported PL of vacuum-deposited thin films of PTCDA on Si(100) and Ag(111).[26-27] In particular, the increase in PL at coverages greater than 3 ML results from the transition from layer-by-layer to Stranski-Krastanov growth of vertical islands of PTCDA, whereby many molecules are beyond the PL quenching distance from the graphene surface.[26,28-32] The existence of a small PL background at 2 ML thickness indicates that our estimated coverage may be slightly lower than the actual thickness.

Recent reports have suggested that optically resonant charge transfer between adsorbed molecules and graphene can lead to a graphene-enhanced Raman signal (GERS) when compared to insulating substrates. Shifts in the optical absorption of molecules adsorbed onto graphene have also been shown to increase the intensity of the Raman signal due to the resonance Raman effect.[33] Preliminary evidence for graphene-enhanced Raman in our studies is provided by the observation that the magnitude of the PTCDA Raman signal relative to the SiC signal decreases with increasing PTCDA thickness. To more rigorously test for GERS, we dosed a single monolayer equivalent of PTCDA onto the wide band gap insulator sapphire. A comparison between the Raman spectra of 1 ML of PTCDA on EG and 1 ML equivalent of PTCDA on sapphire is shown in Figure 2c. On sapphire, a 1 ML dose of PTCDA shows fluorescence (not shown), and the intensity of the 1306 cm^{-1} peak is 85% less than on EG, yielding an effective graphene enhancement factor of 6-7. While it is difficult to pinpoint the mechanism for the enhancement of the Raman signal on graphene as compared to sapphire, we note that the excitation wavelength is still well within the broad absorption band of PTCDA on sapphire (Figure SI-1).

Having established the Raman spectrum of PTCDA on EG, alumina was deposited on the 1 ML PTCDA / EG sample in a Cambridge Nanotech Savannah S100 ALD reactor at 100°C. Control experiments showed that heating the sample to 100°C in the reactor without ALD had no discernible effect on the Raman signal. In an effort to minimize the possibility of mixed monolayer and bilayer patches affecting the results, ALD was also performed on 0.3 ML PTCDA on EG samples. Finally, in order to avoid the effects of inhomogeneity in the submonolayer sample due to the formation of molecular islands, a line scanning confocal Raman system with a 532 nm laser (Raman-11 made by Nanophoton) was used to sample and average over a larger area (90 μm × 12 μm). The Raman spectra taken at 532 nm and 514.5 nm showed similar Raman shifts and intensity distributions for the PTCDA signals, although the relative intensities of the PTCDA bands compared to SiC bands were significantly higher using the Raman-11 system. Additional experimental details related to spectral acquisition can be found in the Supporting Information.

Figure 3 shows the Raman spectra of 0.3 ML PTCDA/EG and 0.3 ML PTCDA/EG after 50 ALD cycles of TMA and H_2O. Previous work[8] has shown that 25 cycles creates a 2 nm thick pinhole-free film with no PTCDA exposed, so 50 cycles represents an excess amount that ensures that any reaction initiated by the PTCDA layer is terminated. Figures 3c and 3d show zoomed-in regions of the Raman spectrum before and after ALD. The low wavenumber region in Figure 3c includes a peak that involves angular distortion of the anhydride group (δC-O-C at 622 cm^{-1}), and the high wave number region in Figure 3d includes a peak from the symmetric carbonyl stretching mode at 1770 cm^{-1}.[34]

Figures 3e and 3f reveal the evolution of the relative intensity and Raman shift of the 1306 cm^{-1} reporter mode. For the first 6 cycles, there is both a reduction in the intensity of the Raman signal, and a slight red-shifting of the aromatic C-H mode at 1306 cm^{-1}. After six cycles, the spectrum has the same shape and intensity as after 50 cycles, thus indicating the

onset of saturation. This observation is slightly more than the four cycles previously reported by Alaboson *et al.* as the number of nucleation cycles required before the ALD growth becomes linear.[8] The reduction in spectral intensity is likely due to the change in the dielectric environment following ALD, in agreement with the lower signal observed for PTCDA on sapphire which has similar dielectric properties to ALD-deposited amorphous alumina.

A one-to-one correspondence exists between the vibrational peaks attributable to PTCDA before and after the ALD process, suggesting that the PTCDA remains molecularly intact following ALD. Previous X-ray reflectivity measurements[8] similarly found that following ALD of alumina on PTCDA/EG, a layer remained on top of the graphene at approximately the same distance from the graphene as pristine PTCDA. These measurements, however, could not confirm the chemical nature of the resulting layer. Furthermore, retention of the δC-O-C and the carbonyl stretching modes indicates that the oxygen atoms in PTCDA do not react directly with TMA to seed growth of alumina. Consequently, we propose an alternate mechanism in which the oxygen atoms in PTCDA serve as hydrogen bonding sites for ambient water molecules up to the ALD growth temperature of 100°C These hydrogen-bonded water molecules then react with TMA to nucleate the ALD alumina film. Future studies will be needed to validate this hypothesis.

The shift in vibrational frequency for the C-H bending mode from 1306 cm^{-1} to 1304 cm^{-1} with increasing ALD coverage provides evidence for a small degree of charge transfer into the PTCDA layer following ALD since this vibration is in plane and thus should be insensitive to the presence of additional mass on top of it. Assuming an average linear shift of −18 e/cm^{-1} and −16 e/cm^{-1} for the cation[15], this would correspond to a charge transfer less than 0.125 electrons. Additional work function measurements could measure this more precisely, as a 2 cm^{-1} shift is close to the experimental resolution. One potential source of charges is the oxide layer itself, which is amorphous and contains a finite density of trapped charges due to vacancies and interstitial substitutions. Another source may be a compression of the PTCDA layer into the graphene following ALD, resulting in stronger substrate-molecule interactions. X-ray reflectivity data show that a pi-stacked layer remains following ALD, although the subsequent peak is asymmetric and shifted to higher q values, indicating a potential compression of up to 0.1 Å.[8] Electrical transport measurements of graphene transistors could potentially distinguish between these two sources of charge transfer. Charges trapped in the oxide layer should increase the hysteresis, while charge transfer from the graphene layer due to compression should alter the location of the Dirac point without altering the hysteresis.

In summary, resonance Raman spectroscopy has been employed to investigate PTCDA seeding layers before and after deposition of alumina by ALD. Through comparative studies on EG and sapphire substrates, the PTCDA signal is found to be enhanced on graphene, providing high sensitivity to PTCDA even at submonolayer coverage. At increasing PTCDA coverage, PL is observed and correlates with thickness beyond the second monolayer, thus providing a rapid screening method for PTCDA thin film growth on graphene. Following ALD of alumina, the Raman spectra reveal that the PTCDA molecules remain molecularly intact, suggesting that ALD is nucleated by water that is hydrogen bonded to the PTCDA. Overall, this study provides insight into the structure and chemistry of PTCDA-seeded ALD growth on graphene, thereby informing future efforts to realize well-defined dielectric-graphene interfaces in electronic and related technologies.

Supplementary Material

Refer to Web version on PubMed Central for supplementary material.

Acknowledgments

This work was supported by the Office of Naval Research (N00014-11-1-0463) and a W.M. Keck Foundation Science and Engineering Grant. J.E.J. acknowledges an IIN Postdoctoral Fellowship and the Northwestern University International Institute for Nanotechnology as well as the National Institutes of Health and National Institute of Arthritis and Musculoskeletal and Skin Diseases (NIH/NIAMS T32 AR007611). J.M.P.A. acknowledges an IBM Ph.D. Fellowship. Public facilities were utilized in the Keck-II Facility of the NUANCE Center at Northwestern University. NUANCE is supported by the NSF-NSEC, NSF-MRSEC, Keck Foundation, State of Illinois, and Northwestern University. Raman experiments were performed in part at the Northwestern University Biological Imaging Facility supported by the NU Office for Research. Confocal Raman microscopy was accomplished with a Nanophoton Raman-11 Microscope generously provided to the Biological Imaging Facility (Northwestern University, Evanston) by Nanophoton Corporation and Left Coast Instruments.

References

(1). Morozov SV, Novoselov KS, Katsnelson MI, Schedin F, Elias DC, Jaszczak JA, Geim AK. Giant Intrinsic Carrier Mobilities in Graphene and Its Bilayer. Phys. Rev. Lett. 2008; 100:016602. [PubMed: 18232798]

(2). Lin Y-M, Dimitrakopoulos C, Jenkins KA, Farmer DB, Chiu H-Y, Grill A, Avouris P. 100-GHz Transistors from Wafer-Scale Epitaxial Graphene. Science. 2010; 327:662. [PubMed: 20133565]

(3). Wang X, Tabakman SM, Dai H. Atomic Layer Deposition of Metal Oxides on Pristine and Functionalized Graphene. J. Am. Chem. Soc. 2008; 130:8152–8153. [PubMed: 18529002]

(4). Xuan Y, Wu YQ, Shen T, Qi M, Capano MA, Cooper JA, Ye PD. Atomic-Layer-Deposited Nanostructures for Graphene-Based Nanoelectronics. Appl. Phys. Lett. 2008; 92:013101.

(5). Ni ZH, Wang HM, Ma Y, Kasim J, Wu YH, Shen ZX. Tunable Stress and Controlled Thickness Modification in Graphene by Annealing. ACS Nano. 2008; 2:1033–1039. [PubMed: 19206501]

(6). Lee B, Mordi G, Kim MJ, Chabal YJ, Vogel EM, Wallace RM, Cho KJ, Colombo L, Kim J. Characteristics of High-k Al_2O_3 Dielectric Using Ozone-Based Atomic Layer Deposition for Dual-Gated Graphene Devices. Appl. Phys. Lett. 2010; 97:043107.

(7). Robinson JA, LaBella M, Trumbull KA, Weng X, Cavelero R, Daniels T, Hughes Z, Hollander M, Fanton M, Snyder D. Epitaxial Graphene Materials Integration: Effects of Dielectric Overlayers on Structural and Electronic Properties. ACS Nano. 2010; 4:2667–2672. [PubMed: 20415460]

(8). Alaboson JMP, Wang QH, Emery JD, Lipson AL, Bedzyk MJ, Elam JW, Pellin MJ, Hersam MC. Seeding Atomic Layer Deposition of High-k Dielectrics on Epitaxial Graphene with Organic Self-Assembled Monolayers. ACS Nano. 2011; 5:5223–5232. [PubMed: 21553842]

(9). George SM. Atomic Layer Deposition: An Overview. Chem. Rev. 2009; 110:111–131. [PubMed: 19947596]

(10). Tian XQ, Xu JB, Wang XM. Self-Assembly of PTCDA Ultrathin Films on Graphene: Structural Phase Transition and Charge Transfer Saturation. Journal of Physical Chemistry C. 2010; 114:20917–20924.

(11). Kaiser R, Friedrich M, Schmitz-Hübsch T, Sellam F, Kampen TU, Leo K, Zahn DRT. Ultra-Thin PTCDA Layers Studied by Optical Spectroscopies. Fresenius J. Anal. Chem. 1999; 363:189–192.

(12). Kampen TU, Salvan G, Tenne D, Scholz R, Zahn DRT. Growth of Organic Films on Passivated Semiconductor Surfaces: Gallium Arsenide Versus Silicon. Appl. Surf. Sci. 2001; 175:326–331.

(13). Scholz R, Kobitski AY, Kampen TU, Schreiber M, Zahn DRT, Jungnickel G, Elstner M, Sternberg M, Frauenheim T. Resonant Raman Spectroscopy of 3,4,9,10-Perylene-Tetracarboxylic-Dianhydride Epitaxial Films. Physical Review B. 2000; 61:13659–13669.

(14). Wagner V, Muck T, Geurts J, Schneider M, Umbach E. Raman Analysis of First Monolayers of PTCDA on Ag(111). Applied Surface Science. 2003; 212-213:520–524.

(15). Kobitski AY, Salvan G, Scholz R, Tenne D, Kampen TU, Wagner HP, Zahn DRT. Raman Spectroscopy of the PTCDA-Inorganic Semiconductor Interface: Evidence for Charge Transfer. Applied Surface Science. 2002; 190:386–389.

(16). Leonhardt M, Mager O, Port H. Two-Component Optical Spectra in Thin PTCDA Films due to the Coexistence of α- and β-Phase. Chem. Phys. Lett. 1999; 313:24–30.

(17). Ling X, Xie L, Fang Y, Xu H, Zhang H, Kong J, Dresselhaus MS, Zhang J, Liu Z. Can Graphene be Used as a Substrate for Raman Enhancement? Nano Lett. 2010; 10:553–561. [PubMed: 20039694]

(18). Wang QH, Hersam MC. Room-Temperature Molecular-Resolution Characterization of Self-Assembled Organic Monolayers on Epitaxial Graphene. Nature Chemistry. 2009; 1:206–211.

(19). Foley ET, Yoder NL, Guisinger NP, Hersam MC. Cryogenic Variable Temperature Ultrahigh Vacuum Scanning Tunneling Microscope for Single Molecule Studies on Silicon Surfaces. Rev. Sci. Instrum. 2004; 75:5280–5287.

(20). Emery JD, Wang QH, Zarrouati M, Fenter P, Hersam MC, Bedzyk M. Structural Analysis of PTCDA Monolayers on Epitaxial Graphene with Ultra-High Vacuum Scanning Tunneling Microscopy and High-Resolution X-ray Reflectivity. J. Surf. Sci. 2011; 605:1685–1693.

(21). Huang H, Chen S, Gao X, Chen W, Wee ATS. Structural and Electronic Properties of PTCDA Thin Films on Epitaxial Graphene. ACS Nano. 2009; 3:3431–3436. [PubMed: 19852489]

(22). Burton JC, Sun L, Pophristic M, Lukacs SJ, Long FH, Feng ZC, Ferguson IT. Spatial Characterization of Doped SiC Wafers by Raman Spectroscopy. J. Appl. Phys. 1998; 84:6268–6273.

(23). Ni ZH, Chen W, Fan XF, Kuo JL, Yu T, Wee ATS, Shen ZX. Raman Spectroscopy of Epitaxial Graphene on a SiC Substrate. Phys. Rev. B. 2008; 77:115416.

(24). Tenne DA, Park S, Kampen TU, Das A, Scholz R, Zahn DRT. Single Crystals of the Organic Semiconductor Perylene Tetracarboxylic Dianhydride Studied by Raman Spectroscopy. Phys. Rev. B. 2000; 61:14564–14569.

(25). Akers K, Aroca R, Hor AM, Loutfy RO. Molecular Organization in Perylenetetracarboxylic Dianhydride Films. J. Phys. Chem. 1987; 91:2954–2959.

(26). Chkoda L, Schneider M, Shklover V, Kilian L, Sokolowski M, Heske C, Umbach E. Temperature-Dependent Morphology and Structure of Ordered 3,4,9,10-Perylene-Tetracarboxylicacid-Dianhydride (PTCDA) Thin Films on Ag(111). Chem. Phys. Lett. 2003; 371:548–552.

(27). Kobitski AY, Salvan G, Wagner HP, Zahn DRT. Time-Resolved Photoluminescence Characterisation of Thin PTCDA Films on Si(100). Appl. Surf. Sci. 2001; 179:209–212.

(28). Gustafsson JB, Moons E, Widstrand SM, Johansson LSO. Thin PTCDA Films on Si(001): 1. Growth Mode Surf. Sci. 2004; 572:23–31.

(29). Gustafsson JB, Moons E, Widstrand SM, Johansson LSO. Growth and Characterization of Thin PTCDA Films on 3C-SiC(001)c(2 × 2). Surf. Sci. 2006; 600:4758–4764.

(30). Kendrick C, Kahn A. Epitaxial Growth and Phase Transition in Multilayers of the Organic Semiconductor PTCDA on InAs(001). J. Cryst. Growth. 1997; 181:181–192.

(31). Kilian L, Umbach E, Sokolowski M. Molecular Beam Epitaxy of Organic Films Investigated by High Resolution Low Energy Electron Diffraction (SPA-LEED): 3,4,9,10-Perylenetetracarboxylicacid-Dianhydride (PTCDA) on Ag(111). Surf. Sci. 2004; 573:359–378.

(32). Stohr M, Gabriel M, Moller R. Investigation of the Growth of PTCDA on Cu(110): An STM Study. Surf. Sci. 2002; 507:330–334.

(33). Thrall ES, Crowther AC, Yu Z, Brus LE. R6G on Graphene: High Raman Detection Sensitivity, Yet Decreased Raman Cross-Section. Nano Lett. 2012; 12:1571–1577. [PubMed: 22335788]

(34). Kobitski AY, Scholz R, Zahn DRT. Theoretical Studies of the Vibrational Properties of the 3,4,9,10-Perylene Tetracarboxylic Dianhydride (PTCDA) Molecule. J. Mol. Struct.: THEOCHEM. 2003; 625:39–46.

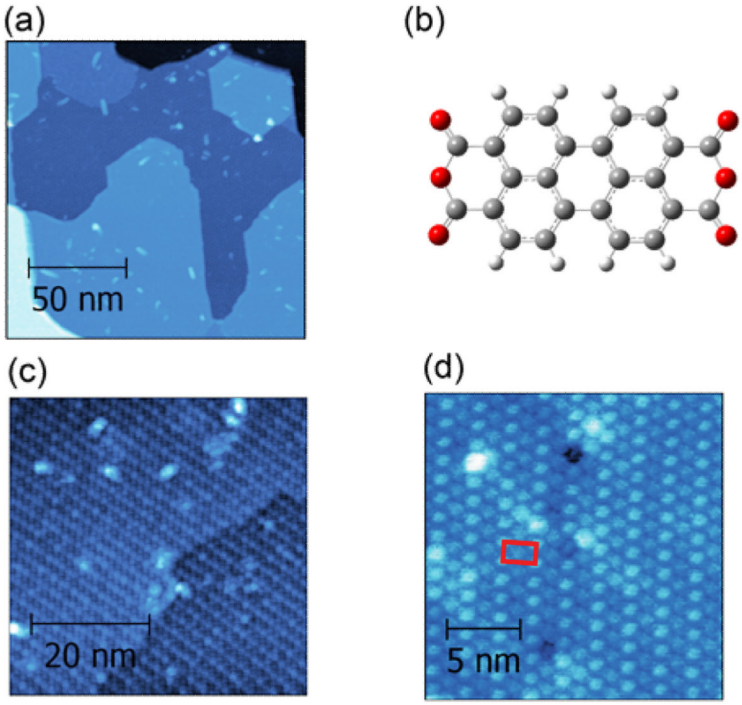

Figure 1.
Constant current UHV STM images showing the structure of PTCDA on epitaxial graphene (EG). (a) STM image of as-prepared EG, showing patches of monolayer and bilayer graphene with one-dimensional and point defects on the surface (tunneling current = 60 pA and sample bias = −2.0 V). (b) Molecular structure of PTCDA (gray = carbon; red = oxygen; white = hydrogen). (c) PTCDA self-assembles in a herringbone structure that smoothly coats step edges and defects (50 pA and −1.0 V). (d) High-resolution STM image showing the unit cell in red (40 pA and −1.0 V). The slight bend to the right of the PTCDA lattice can be attributed to thermal drift and/or piezoelectric creep during imaging.

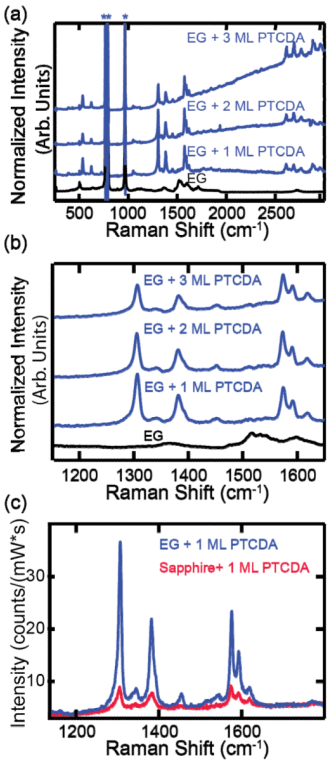

Figure 2.

Raman spectra of PTCDA at an excitation wavelength of 514.5 nm. (a) Raman spectra of 0 to 3 monolayers (ML) of PTCDA on epitaxial graphene (EG). Spectra are intensity-normalized to the substrate peak at 788 cm^{-1}. Increasing coverage beyond the second monolayer of PTCDA leads to the onset of a fluorescence background. The three features marked with an asterisk are the primary Raman peaks of the SiC substrate. (b) Zoomed-in region of (a) showing the most intense peaks that have been attributed to the motion of the aromatic hydrogens and sp^2 carbon-carbon stretches. The intensities in (a) and (b) are normalized to the most intense SiC peak at 788 cm^{-1} and offset for clarity. (c) Raman spectra of 1 ML equivalent of PTCDA deposited on EG and sapphire taken under identical conditions. The Raman signal is 6-7 times stronger on EG than on sapphire.

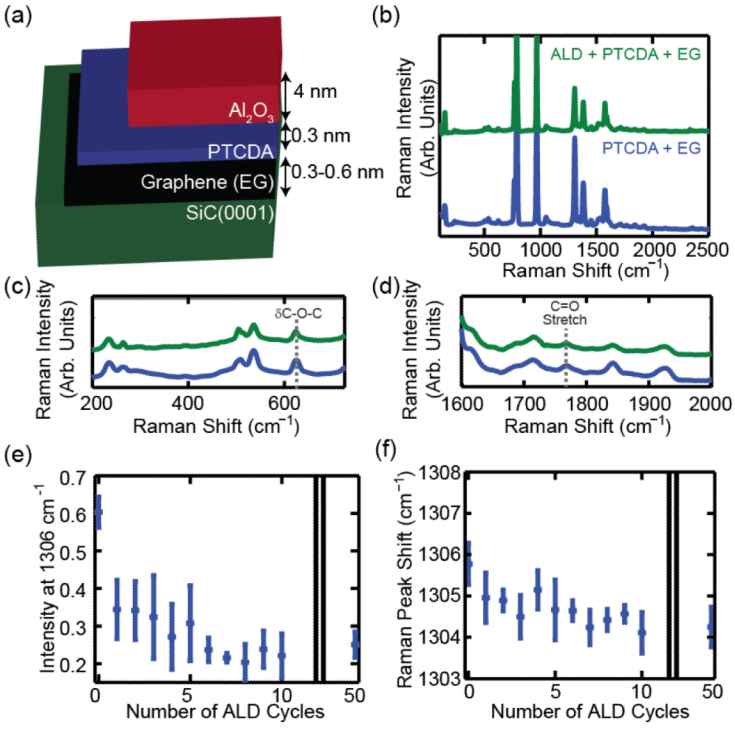

Figure 3.

(a) Schematic of the final thin film structure after 50 cycles of alumina atomic layer deposition (ALD). (b) Raman spectra taken at 532 nm for PTCDA on epitaxial graphene (EG) before (blue) and after (green) 50 ALD cycles of TMA and H_2O. All of the PTCDA vibrations observed for PTCDA on EG are still present following ALD. (c) and (d) are zoomed-in portions of the Raman spectra showing the persistence of weaker peaks after ALD. In particular, the symmetric C=O stretch at 1772 cm^{-1} and the motion of the anhydride at 622 cm^{-1} survive the deposition, indicating that they are not directly involved in bonding to the ALD alumina film. (e) and (f) Cycle-by-cycle intensity and peak shift of the most intense peak at 1306 cm^{-1}, revealing that the spectrum has converged to its final value within ~ 6 ALD cycles. All spectra are intensity normalized to the most intense SiC peak at 788 cm^{-1} and vertically offset for clarity. Error bars represent the standard deviation of measurements taken in multiple locations on the sample.

Table 1

Measured frequencies of a PTCDA monolayer adsorbed on epitaxial graphene (EG).

Single Crystal Reference Frequency (cm^{-1})[a]	Monolayer PTCDA Frequency on EG (cm^{-1})	Relative Intensity
232.9	231	0.24
262.2, 259.3[b]	261	0.03
387.6, 388.2[b]	389	0.03
430	428	0.01
538.6, 539.1[b]	535	0.4
623.3, 625.6[b]	622	0.32
725.7	725	0.10
1300.6	1301	0.34
1302.3	1306	1
1344.0	1345	0.11
1381.8	1381	0.43
1383.6	1384	0.21
1451	1448, 1454[b]	0.04, 0.05
1570	1573	0.53
1589	1591	0.283
1615	1615	0.08
1783	1772	0.01

[a] Reference vibrational frequencies are taken from the single crystal measurements of Tenne *et al.*[24]

[b] Multiple mode entries on a single line are Davydov splittings that are only reported here or in the single crystal experiment.